

Review

# Eyeing up the Future of the Pupillary Light Reflex in Neurodiagnostics

Charlotte A. Hall and Robert P. Chilcott \*

Research Centre for Topical Drug Delivery and Toxicology, University of Hertfordshire, Hatfield SP10 1JX, UK; c.hall5@herts.ac.uk

\* Correspondence: tox.publications@herts.ac.uk; Tel.: +44-(0)7718696629

Received: 22 February 2018; Accepted: 12 March 2018; Published: 13 March 2018

**Abstract:** The pupillary light reflex (PLR) describes the constriction and subsequent dilation of the pupil in response to light as a result of the antagonistic actions of the iris sphincter and dilator muscles. Since these muscles are innervated by the parasympathetic and sympathetic nervous systems, respectively, different parameters of the PLR can be used as indicators for either sympathetic or parasympathetic modulation. Thus, the PLR provides an important metric of autonomic nervous system function that has been exploited for a wide range of clinical applications. Measurement of the PLR using dynamic pupillometry is now an established quantitative, non-invasive tool in assessment of traumatic head injuries. This review examines the more recent application of dynamic pupillometry as a diagnostic tool for a wide range of clinical conditions, varying from neurodegenerative disease to exposure to toxic chemicals, as well as its potential in the non-invasive diagnosis of infectious disease.

**Keywords:** pupillometry; acetylcholine; cholinergic system; neurodegeneration; trauma; infection; recreational drugs; chemicals; toxins; autism

---

## 1. Introduction

The origin of the phrase “the eyes are the window to the soul” is attributed to the Roman Consul Cicero, but during the past three decades the ability of the eye to act as a window into nervous system function has been exploited for a wide range of clinical applications, including mental health and neurodegenerative disorders, as well as exposure to toxic or illicit substances and trauma.

The pupillary light reflex (PLR) describes the constriction and subsequent dilation of the pupil in response to light, which not only serves as a major determination of retinal image quality [1,2], but also provides an important metric of autonomic nervous system function [3]. As such, measurement of the pupil’s response to light serves as a non-invasive tool for basic neuroscience research and the study of parasympathetic and sympathetic balance.

## 2. Pupillary Light Reflex

The pupil has a large dynamic range, typically from 7.5–8 mm diameter at full mydriasis to 1.5–2 mm diameter at full miosis, and is controlled by the antagonistic actions of the iris sphincter and dilator muscles [4]. The sphincter and dilator are innervated by the parasympathetic and sympathetic nervous systems, respectively; thus, different parameters of the PLR can be used as indicators for either sympathetic or parasympathetic modulation. Factors which affect average pupil diameter include age, sex, iris colour, retinal and optic nerve health and optical media clarity [5]; however, the most powerful determinant of pupil size is ambient light level.

### 3. Measuring the PLR

The dynamics of the PLR follow a general pattern consisting of 4 phases: response latency, maximum constriction, pupil escape and recovery (Figure 1), which can be influenced by the duration, intensity and spectral composition of the light. The PLR provides a physiological measure of normal or abnormal nervous system function and the symmetry of the PLR in response to stimulation of either eye, because of pupillary fibre decussation, provides an opportunity to compare the pupillomotor drive in both eyes [6].

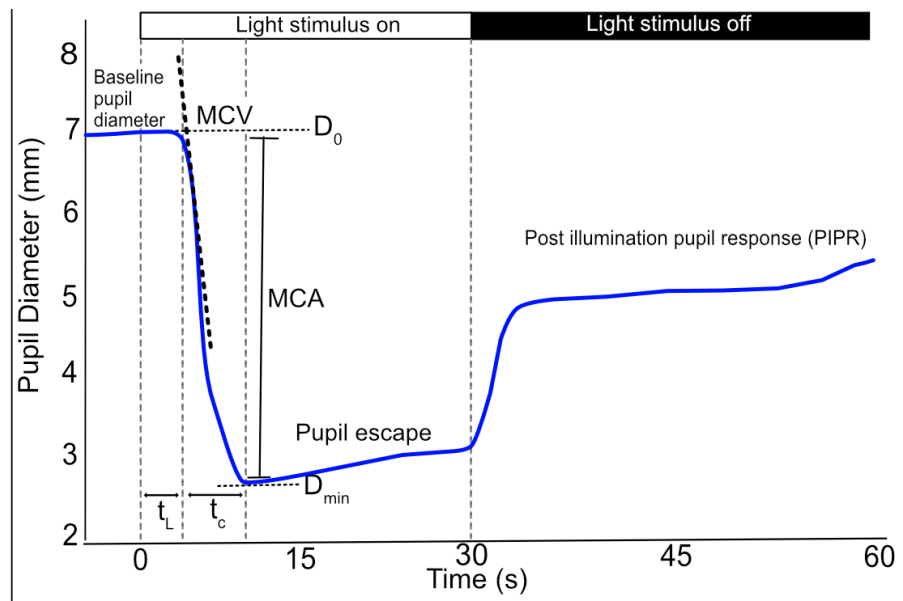


**Figure 1.** Schematic of the pupillogram (blue line) and associated PLR parameters. The light stimulus at time zero results in a rapid reduction in pupil diameter. Latency ( $t_L$ ) is calculated as the elapsed time between light onset and the start of constriction. The pupil then rapidly constricts (maximum constriction velocity; MCV) from the baseline ( $D_0$ ) pupil diameter to the minimum ( $D_{min}$ ) pupil diameter; the constriction time ( $t_c$ ) and maximum constriction amplitude (MCA) are calculated as the time interval and size difference between these two values, respectively. At offset of light stimulus or during sustained light stimulation the pupil undergoes a period of rapid redilation or pupillary “escape” to a partially constricted state. Subsequently the pupil slowly returns to the baseline diameter.

Response latency describes the delay in pupil constriction following the onset of a light stimulus, with the latency shortening as light intensity increases, to a minimum of 180–230 ms [7,8]. The latency period is due to the delay in iris smooth muscle contraction and to a lesser extent the temporal dynamics of retinal output and innervation pathways [7,8].

The latency period is followed by a period of rapid constriction of the pupil until it reaches the maximum constriction velocity (MCV), after which constriction slows until the minimum pupil diameter is reached. The onset of pupil contraction can be determined using velocity and acceleration analysis [9]. The maximum constriction velocity varies with light stimulus intensity, duration, spectral composition, retinal size and location [10]. The maximum constriction amplitude (MCA) represents the difference between the baseline and minimum pupil diameter. However, the baseline pupil diameter can be affected by a number of factors and can influence the MCA (a smaller MCA is observed with a smaller baseline pupil diameter). Therefore, the MCA should be normalised to baseline pupil diameter to account for this effect [6]. After this peak constriction, the pupil quickly redilates or “escapes” to a partially constricted state during a prolonged light stimulus lasting from 1–2 up to 100 s, before slowly redilating to the initial size [11].

In addition to the dynamic phases of the PLR during light stimulation, there is also a sustained component [12,13]. Both outer and inner photoreceptors contribute to the early sustained post-illumination pupil response (PIPR; <1.7 s post-stimulus) [14]. Subsequently, the PIPR, which may be sustained for up to 3 minutes after light offset depending on the properties of the light stimulus, is solely controlled by the intrinsically photosensitive retinal ganglion cells that depolarise during light stimulation (dependent on both light intensity and wavelength) and then repolarise slowly after light offset [6,13–15].

The response of the pupil to light can be manually assessed using the swinging flashlight test or using a pupillometer device. Pupillometers enable objective quantification of the PLR and generally consist of an infrared-sensitive imaging sensor coupled with a digital interface for the automated recording, processing and reporting of pupil data. The acquired images are processed to yield a pupillogram with pupil size plotted as a function of time, from which PLR parameters can be calculated (Figure 1). There are several commercially available pupillometers and the relative performance of commercial systems is the subject of several publications [16–18]. However, commercial systems are typically designed for specific applications and use proprietary software, which may limit their use for basic research. In response, a number of research groups have published methods for developing prototype automated infrared pupillometers, which use open-source software [19,20]. There is also increasing use of remote eye-tracking devices, such as Tobii, that are capable of measuring pupil size and can be used in combination with open-source software for the analysis of PLR [21].

## 4. Neuronal Basis for the Pupillary Light Reflex

### 4.1. Pupil Constriction

There are three major divisions of parasympathetic neurons that integrate the light stimulus to produce a pupil contraction: (i) an afferent division; (ii) an interneuron division; and (iii) an efferent division. The response latency, maximum constriction and pupil escape, and the corresponding constriction parameters (MCV, MCA and RCA; relative constriction amplitude) are dependent on the actions of the sphincter muscle and on the function of retinal photoreceptors, as well as the time consumed in the afferent and efferent pathway. They are thus under direct control of the parasympathetic nervous system. Both MCV and RCA parameters are dependent on the baseline pupil diameter in healthy individuals and it is important to normalise measurements with respect to baseline values [6,22]. There is also a strong linear relationship between MCV and MCA [20]; thus, MCV and RCA are considered to be the most robust parameters for detecting parasympathetic dysfunction [23].

### 4.2. Afferent Arm of Pupil Constriction

The afferent limb of the PLR begins with photoreceptive inputs from rod, cone and intrinsically photosensitive retinal ganglion cells (ipRGCs) located in the retina (summarised in Figure 2).

Under dark conditions, rod and cone photoreceptors exist in a constant depolarised state and continuously release glutamate [24,25]. However, when stimulated by light, the rod and cone photoreceptors undergo graded alterations in membrane potential and hyperpolarize, resulting in a reduction in glutamate release. Rod and cone cells synapse with their respective bipolar cells and reductions in glutamate release results in either inhibition or disinhibition of the bipolar cells depending on whether they express excitatory ionotropic (“ON”) or inhibitory metabotropic (“OFF”) glutamate receptors [26]. These “ON” or “OFF” bipolar cell subtypes synapse with the corresponding retinal ganglion cell (RGC) in the non-cholinergic regions of the inner plexiform layer (IPL). Horizontal neurotransmission also occurs within the IPL and outer plexiform layer (OPL) via amacrine and horizontal cells, respectively, and is critical in shaping the spatial and temporal aspects of photopic and scotopic vision [27].

The third photoreceptor, ipRGC, accounts for approximately 1% of the total RGCs [28–30]. These cells have a role in non-image-forming visual processes, such as circadian photoentrainment,

as well as in the PLR [31–33]. The ipRGCs regulate pupil size through the integration of extrinsic signals from rods and cones but also through intrinsic (melanopsin) phototransduction [12]. Melanopsin is a G protein-coupled photopigment, which is maximally sensitive to 482 nm wavelength light and, unlike rods and cones, depolarizes in response to light following activation of a phototransduction cascade involving Gq/11 and phospholipase C [34–37]. Unlike rods and cones, which have their photopigment concentrated in specialised light-absorbing cellular domains (outer segment), melanopsin is distributed throughout the plasma membrane of ipRGCs [28]. The ipRGCs also directly contribute to the PIPR as a sustained constriction of the PLR (>30 s) in response to high intensity, short wavelength light [14,15,28,38–40].

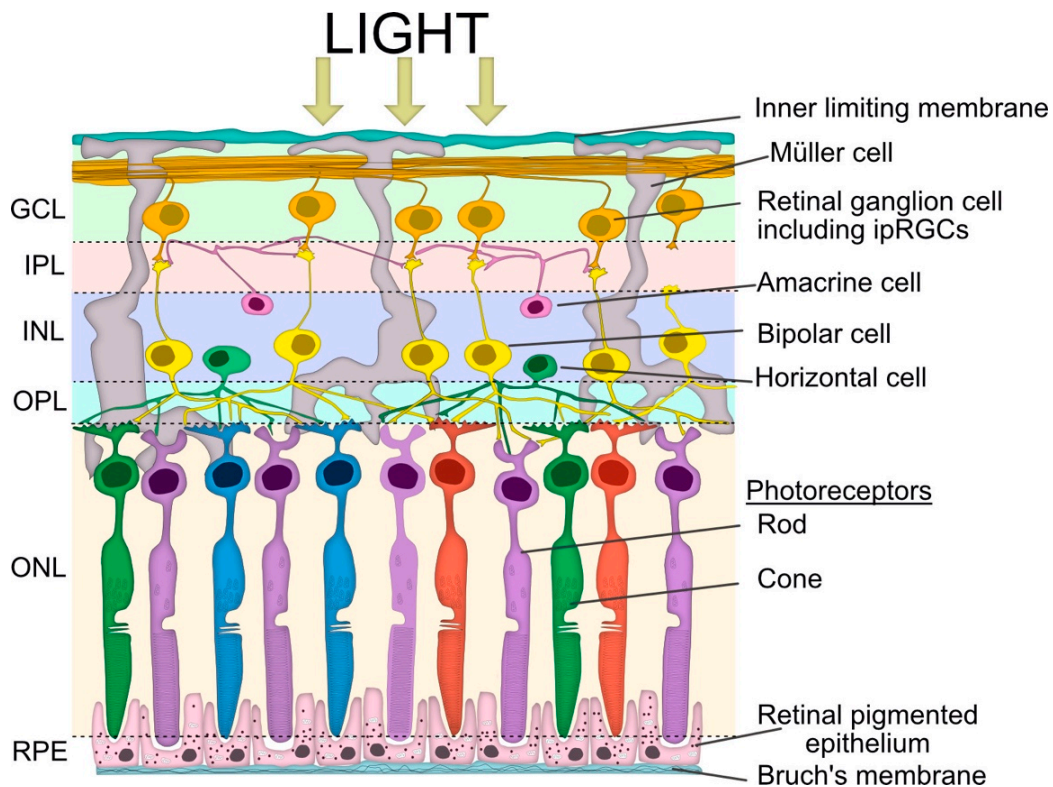


**Figure 2.** Simplified schematic view of retinal layers involved in the pupillary light reflex. Vertical signalling pathways in the retina are composed of the photoreceptors (rod and cone cells), bipolar cells and retinal ganglion cells (RGC), including intrinsically photosensitive retinal ganglion cells (ipRGCs). There are also two lateral pathways comprised of horizontal cells in the outer plexiform layer (OPL) and the amacrine cells in the inner plexiform layer (IPL). These cells modulate the activity of other retinal cells in the vertical pathway. The somata of the neurons are in three cellular layers. The rod and cone cells are located in the outer nuclear layer (ONL), which is adjacent to the retinal pigment epithelium (RPE). The horizontal cell, bipolar cell and amacrine cell somata are located in the inner nuclear layer (INL), whilst the ganglion cell somata are located in the ganglion cell layer (GCL). The axon terminals of the bipolar cells stratify at different depths of the inner plexiform layer, which is subdivided into the OFF outer sublamina (where OFF bipolar cells terminate) and the ON inner sublamina (where ON bipolar cells terminate). There are also ON and OFF bands of melanopsin dendrites from the ipRGCs, but both lie outside of the ON and OFF cholinergic bands within the IPL. The bipolar cells are photoreceptor specific and the bipolar dendrites synapse exclusively with either rod or cone cells.

### 4.3. The Interneuron and Efferent Arms of Pupil Constriction

The interneuron and efferent arms of pupil constriction are summarised in Figure 3. The RGC axons form the first interneuron arm of the PLR arc and carry the neuronal signal from the photoreceptors [2].

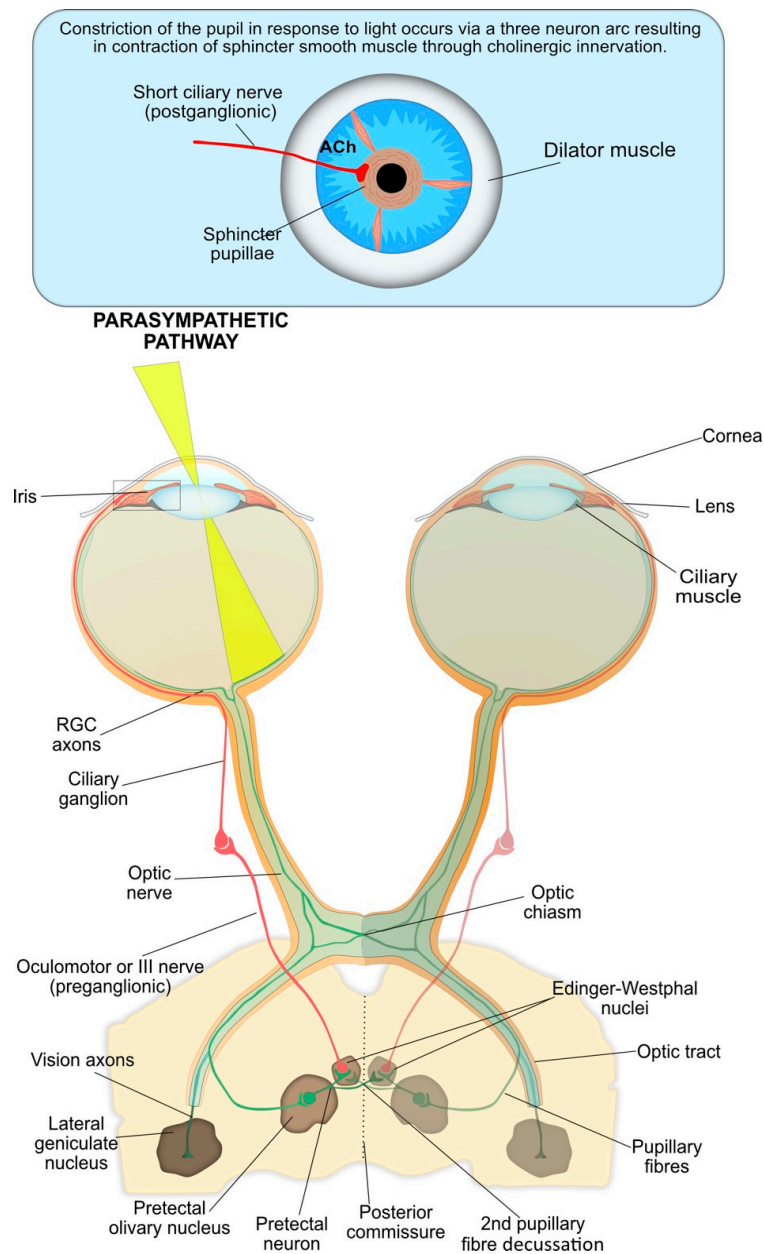


**Figure 3.** The parasympathetic nervous system is the main system responsible for pupil constriction in response to light. The integrated afferent input is transmitted along the axons of the retinal ganglion cells (RGC), which contribute to the optic nerve. At the optic chiasm, nerves from the nasal retina cross to the contralateral side, whilst nerves from the temporal retina continue ipsilaterally. The pupillary RGC axons exit the optic tract and synapse at the pretectal olivary nucleus. Pretectal neurons are projected either ipsilaterally or contralaterally, across the posterior commissure, to the Edinger-Westphal nucleus. From there, the pre-ganglionic parasympathetic fibres travel with the oculomotor, or III cranial nerve, and synapse at the ciliary ganglion. The post-ganglionic parasympathetic neurons (short ciliary nerves) travel to and innervate the contraction of the iris sphincter muscle via the release of acetylcholine at the neuromuscular junction, resulting in pupil constriction.



At the optic chiasma, approximately half the RGCs from the nasal plane in each eye decussate to the opposite optic tract [41]. At the terminus of the optic tract, the axons of RGCs responsible for the PLR separate from the visual axons and carry the afferent pupillomotor signal through the brachium of the superior colliculus to synapse at the pretectal olivary nucleus in the dorsal midbrain [8].

The pretectal neurons integrate the input signals (retinal, supranuclear and infranuclear), that modulate the PLR and form the second interneuron of the reflex arc. These pretectal nuclei project to either the ipsilateral or contralateral Edinger–Westphal (EW) nucleus within the oculomotor nuclear complex, which contain the pre-ganglionic parasympathetic neurons that control the iris sphincter [42]. The bilateral neuron projection results in a double decussation of pupillary fibres, first at the optic chiasm and then within the pretectal area, and ensures each EW nucleus receives information about the level of incoming light from each eye. Therefore, unilateral light stimulation causes an equal direct and consensual pupillary constriction. However, contraction anisocoria, whereby the direct pupillary constriction is slightly stronger than the consensual reaction, may present if asymmetry occurs during crossing of fibres at the chiasm or pretectal olivary nucleus; this is normally clinically insignificant [8].

From the EW nuclei, the efferent pre-ganglionic axons pass into the right and left fascicles of the oculomotor nerve (third nerve) to join the motor axons destined for the eye muscles (Figure 3). The oculomotor nerve bifurcates into a superior and inferior division near the anterior cavernous sinus. The parasympathetic fibres travel with the inferior division through the superior orbital fissure toward the orbital apex and synapse at the ciliary ganglion (CG).

The short ciliary (post-ganglionic) nerves pierce the globe around the optic nerve and pass between the choroid and sclera toward the iris. These nerves innervate the contraction of the iris sphincter muscle via the neurotransmitter acetylcholine (ACh), resulting in constriction of the pupil.

#### 4.4. Pupil Reflex Dilation: Central and Peripheral Nervous System Integration

Dilation of the pupil following a light stimulus occurs through two integrated processes driven by the sympathetic neurons and corresponds to the recovery phase of the PLR and is summarised in Figure 4. Firstly, the parasympathetic innervation of the pupil sphincter is suppressed by supranuclear inhibition via central sympathetic neurons, resulting in relaxation of the muscle and pupil dilation. These sympathetic neurons primarily originate in the reticular activating formation in the brainstem and inhibit the pre-ganglionic parasympathetic neurons at the EW nucleus via  $\alpha_2$ -adrenergic receptor activation. Secondly, the iris dilator muscle contracts via excitation of the  $\alpha_1$ -adrenergic sympathetic pathway. This peripheral sympathetic nerve activation greatly enhances the dynamics of pupil dilation in terms of speed and maximal pupil diameter attained.

The sympathetic influence on the iris dilator muscle consists of a paired, three-neuron arc on both the right and left side of the central and peripheral nervous system, without decussations, extending from the hypothalamus to the iris dilator muscle (Figure 4) [43–45]. In this three-neuron arc, the synaptic transmission is mediated by ACh at the first two junctions, while the post-ganglionic fibres innervate the dilator muscle via noradrenaline.

#### 4.5. Other Inputs to the Iris

Nerves within the ophthalmic division of the trigeminal nerve provide sensory innervation to the iris and may play an additional role in modulating pupil diameter [46]. Mechanical and chemical irritation of the eye can cause a strong miotic response that is non-cholinergic and fails to reverse with autonomic-acting drugs. In addition to the neuronal mechanisms involved in pupil size control, circulating catecholamines and peptide hormones may act on the iris dilator or sphincter muscles, either directly through the bloodstream or potentially indirectly through the tears [47,48].

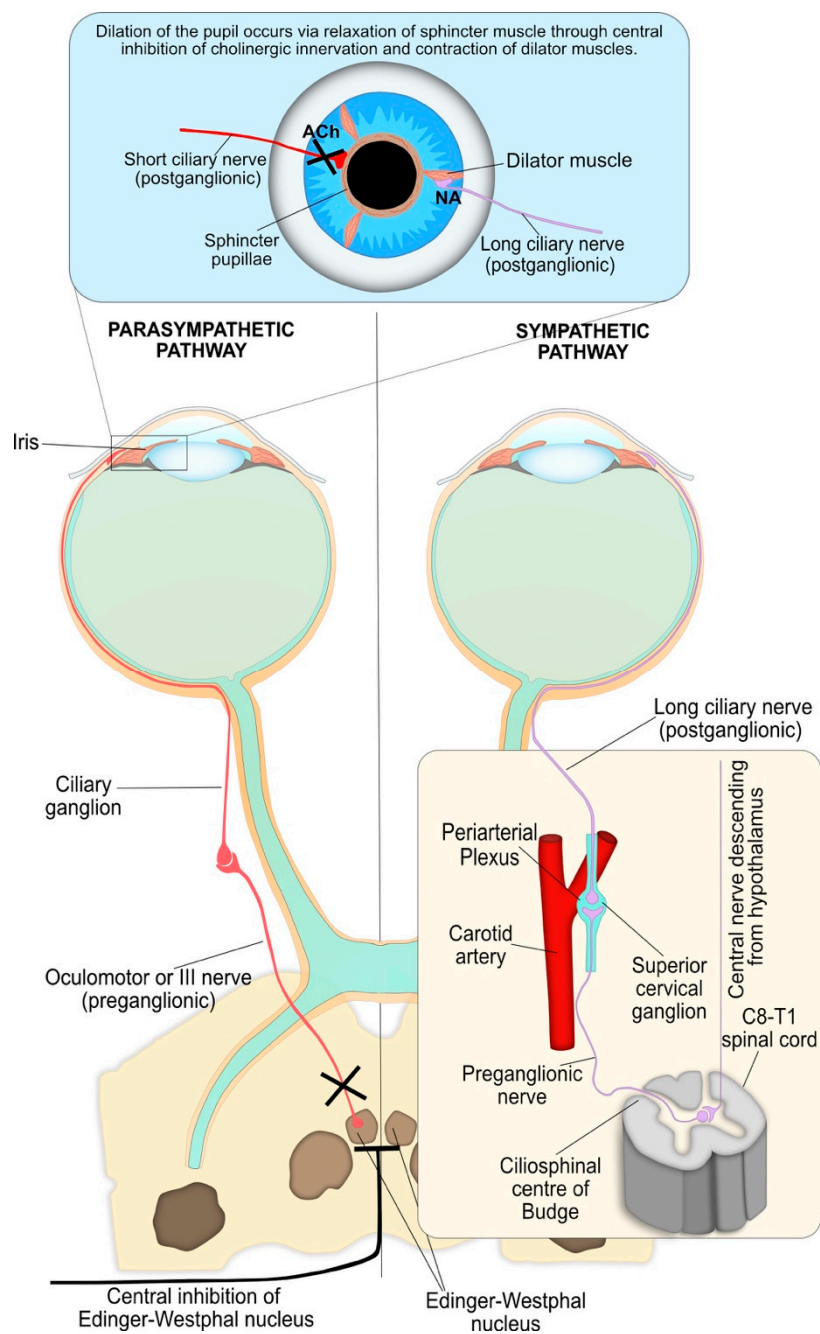


**Figure 4.** Both parasympathetic and sympathetic nervous systems are required for pupil dilation as part of the PLR. The parasympathetic innervation of the pupil sphincter is inhibited by central supranuclear inhibition of Edinger–Westphal nuclei via  $\alpha_2$ -adrenergic receptor activation, resulting in relaxation of the pupil sphincter muscle. The sympathetic influence on the iris dilator muscle consists of a paired three-neuron arc on both the right and left sides of the central and peripheral nervous system without decussations. The first-order (central) neuron originates in the hypothalamus and descends to synapse with the pre-ganglionic in the ciliospinal centre of Budge at C8–T1 of the spinal cord. The pre-ganglionic neuron ascends from the ciliospinal centre of Budge to synapse with the post-ganglionic neuron at the superior cervical ganglion, which is located at the periarterial plexus near the carotid artery bifurcation. Finally, long ciliary (post-ganglionic) nerves travel to and innervate the contraction of the iris dilator muscles, via a release of noradrenaline (NA) at the neuromuscular junction, resulting in pupil dilation. The synaptic transmission at the other junctions is mediated by acetylcholine.

## 5. Clinical Applications of Pupillometry

Conditions that influence the integration of parasympathetic stimulation and inhibition, sympathetic stimulation and humoral release of neurotransmitters may each affect the dynamics of the PLR and may be clinically diagnostic. Pupil function abnormalities have been reported for a wide range of disorders, including alcoholism [49,50], mental health disorders such as seasonal affective disorders [51], schizophrenia [52] and generalised anxiety disorder [53], Alzheimer's [54–56] and Parkinson's [57–60] diseases, autism spectrum disorders [61,62], as well as glaucoma [14,63–65] and autonomic neuropathies associated with diabetes [66–70]. Additionally, pupillometry has been applied to other clinical fields, such as monitoring of central states in anaesthesiology and analgesia, as well as monitoring and prognosis following head injuries, cardiac arrest and drug overdose [71].

### 5.1. Neurodegenerative Disorders

There is an established body of evidence to indicate that cholinergic hypofunction is a significant component of neurodegenerative diseases, such as Alzheimer's and Parkinson's diseases, which are due to ACh and dopamine deficiencies, respectively. Moreover, the majority of studies that analysed ACh-dependent PLR parameters have revealed significant differences between normal age-matched patients and those with Alzheimer's [55–57,72–74] or Parkinson's disease [58,59,75]. Studies typically used light stimuli wavelength of 820 nm with a light intensity of 24.6 cd/m<sup>2</sup>. Specifically, patients with Alzheimer's [57] or Parkinson's disease, with or without any detectable cognitive deficits or psychiatric disorders [55,57,75], had significantly lower MCV and MCA values. Ferrario et al. [76] did not observe a significant difference in MCA between Alzheimer's patients and controls; however, this may be attributed to the longer light stimulus used (1 s) compared to the other studies (20–150 ms) [77].

The MCV and MCA parameters correspond to the first portion of the characteristic V-shaped pupillometric response (Figure 4) and are considered the most sensitive markers of cholinergic activity [78]. Therefore, the MCA and secondarily the MCV are the best PLR predictors to discriminate between healthy individuals and patients with Alzheimer's or Parkinson's disease [57,72]. A significant increase in latency has been observed for subjects with Parkinson's disease [57–59]; however, this was not observed consistently in those with Alzheimer's disease [54,56,72]. Additionally, Bittner et al. examined the pupil's response under repetitive light stimulation, which is systematically unstable in normal patients [54]. However, these changes were not observed in patients with Alzheimer's disease.

A number of possible pathophysiological mechanisms have been proposed for the observed changes in pupillary response seen in Alzheimer's and Parkinson's patients [60], but Fotiou et al. [57] and others have concluded that the most significant factor behind these findings was likely to be the involvement of a central cholinergic deficit. Pupillometry, including repeated light stimulation pupillometry, may serve as a useful diagnostic tool even at early, subclinical stages of autonomic nervous system dysfunction [57,58].

### 5.2. Trauma

The PLR is a well-established measurement in the management and prognosis of patients with acute brain injuries, in conjunction with other clinical parameters such as age, mode of injury and Glasgow Coma Scale [79–81]. Typical light stimuli parameters are a 465 nm wavelength with a duration of 1 s and low luminance (0.001 cd/m<sup>2</sup>) used to stimulate rod cells or high luminance (450 cd/m<sup>2</sup>) used to stimulate ipRGCs. In particular, the location of the pupillomotor nuclei within the dorsal midbrain and efferent oculomotor nerve are important in the determination of brainstem compression and the onset of transtentorial herniation [82]. Morris et al. reported that loss of the PLR or development of anisocoria or pupil asymmetry >2 mm in patients who sustained traumatic brain injuries was correlated with increased morbidity and mortality rates [83]. However, manual examination using a penlight is subject to large inter-examiner discrepancies that can be as high as 40%, particularly when pupils are constricted [84], and these may be further confounded by a variety of factors, including alcohol,



narcotics or hypothermia, which are common to many trauma patients [85]. Furthermore, Couret et al. observed an error rate of approximately 20% even for intermediate-sized pupils (2–4 mm), with a 50% failure rate in the detection of anisocoria [86]. Additionally, Larson and Muhiudeen found complete failure in the detection of the PLR by manual examination when the reflex amplitude was less than 0.3 mm [87]. Automated pupillometry using a pupillometer is a more sensitive technique that has smaller inter-examiner discrepancies compared to manual examination [86,88]. The ability of pupillometry to detect subtle changes in pupillary reaction even when pupils are constricted has potential clinical significance and may provide a useful tool in the early detection, monitoring and management of brain injuries [89]. In support of this, several groups have demonstrated that use of a pupillometer was superior to manual assessment in predicting the 90-day outcome following cardiac arrest [90,91].

### 5.3. Autism

The cholinergic system is key to normal pre- and postnatal neurodevelopment, and numerous studies, ranging from neuroimaging data [92], to post mortem histopathological analysis of brain tissue [93,94], animal models [95,96] and molecular genetic studies [97], have suggested that alterations in the cholinergic system may be a contributing factor to the aetiology of autism spectrum disorder (ASD). Moreover, an atypical PLR is reported in both children and adults with ASD [60,98–100].

Common measurement parameters used include a light stimulus wavelength of 530 nm and a duration of 100 ms with a light intensity of 63.1 cd/m<sup>2</sup>. Typically, these differences are characterised by longer latency, reduced constriction amplitude [61,99] and reduced constriction velocity [61] compared to children without ASD. However, Nyström et al. reported the opposite for high ASD-risk infants, defined as those who had a sibling with ASD. The difference in age among the studies' subjects, who ranged from 10-month-old infants [100] up to children >5 years of age [61,98,99], may provide an explanation for the contrasting data.

Children without ASD exhibit an age-dependent decrease in PLR latency before reaching a plateau at >8 years of age [98,99]; this correlates with similar trends in white-matter maturation rates as determined by flash visual evoked potential studies [101]. However, in children with ASD there was no age-dependent decrease in PLR latency [99]. Moreover, brain-imaging studies have shown that the neurodevelopment trajectory of brain maturation is atypical in children with ASD. Initially, young children (<4 years of age) exhibit accelerated maturation and a larger brain volume compared to children without ASD [102–106], but this is followed by a period of arrested maturation after 4 years of age [104,107], and then a possible decrease in brain volume in older children and adults [108]. Therefore, the hypersensitive PLR observed in infants with a high risk of ASD [100] could be attributed to the accelerated white-matter maturation associated with ASD, which then reverses after 4 years of age, resulting in a hyposensitive PLR response corresponding to the reduction in PLR parameters [61,98,99].

There is evidence to suggest that, apart from the cholinergic system, other neurotransmitter systems are altered in ASD, such as glutamatergic and GABAergic transmission [109]. Therefore, the PLR may also be affected as a result of altered bipolar cell signalling within the retina. Overall, assessment of the PLR by pupillometry may provide a rapid and non-invasive diagnostic tool for infants and children with a high risk of ASD or other cholinergic-dependent neurological development disorders [100].

### 5.4. Alcohol and Recreational Drugs

Pupillometry offers a reliable and convenient tool for illicit drug and alcohol screening [110–112]. A number of studies have demonstrated the ability of pupillometry to differentiate between potentially drug impaired and normal subjects with 70–100% accuracy [113,114]. The most significant parameters were RPA and MCV [112]. Additionally, pupillometry may offer benefits over urinalysis, particularly in the case of roadside testing, as it provides a measurement of function and impairment rather than

a measurement of drug metabolites, which may be present in the urine for an extended period even though any drug-induced physiological effects or impairment have ceased.

#### 5.4.1. Alcohol

Pupillometry may have a role in both the detection of alcohol intoxication and treatment management during alcohol withdrawal. Data from chromatic pupillometry studies demonstrated a significant increase in both baseline pupil diameter and peak constriction amplitude following a 600 nm wavelength light stimulus at exhaled breath alcohol concentrations of  $\geq 0.25$  mg/L [115]. However, following a high dose of alcohol (1 g/kg body weight) the opposite was observed, with significant decreases in pupil diameter, constriction amplitude and velocity compared to control groups, suggesting inhibition of parasympathetic nerve activity [116,117]. These apparently contradictory results are likely to reflect the acute, dose-dependent inhibition of the parasympathetic nervous system, which results in the predominance of sympathetic nerve activity [118].

Pupillometry may also have a role in the development of clinical management tools to prevent severe autonomic dysfunction during alcohol withdrawal [119]. Specifically, prolonged latency and decreased constriction velocity parameters were described for participants undergoing alcohol withdrawal. The reduction in parasympathetic innervation of the pupil is likely to be due to increased activation of the locus coeruleus, as previously described during alcohol withdrawal [120,121].

#### 5.4.2. Recreational Drugs

The pupillary response to 3,4-methylenedioxymethamphetamine (MDMA) and tetrahydrocannabinol (cannabis) is characterised by an indirect central parasympathetic inhibition, resulting in significantly increased latency and decreased constriction amplitude and velocity [113,122,123]. Additionally, increased sympathomimetic activity due to increased noradrenaline and serotonin signalling was reported following MDMA intoxication, resulting in mydriasis and a reduction in the PLR recovery time [123].

However, for cannabis intoxication there are conflicting reports regarding the effect of the drug on baseline pupil diameter. Hartman et al. observed a significantly increased pupil size compared to control participants, under both scotopic and photopic light conditions as well as following direct light stimulation, suggesting increased sympathetic nervous system activity [112]. This is in contrast to data reported by Fant et al. and others, which demonstrated a significant cannabis-induced effect on the PLR but either a small (0.5 mm) decrease [116,124] or no change [122] in baseline pupil diameter. These differences may be attributed to study design, as the studies that observed little or no effect on pupil diameter used a defined, high dose (27 mg  $\Delta^9$ THC) and a specified time duration between drug administration and pupil measurements, whereas Hartman et al. used Drug Recognition Expert examination data; thus, the exact dose and timings are undefined [113,116,122].

#### 5.5. Exposure to Toxins and Toxic Chemicals

Changes in pupil size and response to light have been reported following exposure to toxic chemicals such as organophosphates, as well as bacterial toxins including botulinum toxin.

Ophthalmic manifestations are early and persistent signs of botulism. Botulinum toxins (BTx) block the release of ACh at neuromuscular junctions, post-ganglionic parasympathetic nerve endings, and post-ganglionic sympathetic nerve endings that release ACh, resulting in paralysis of the sympathetic and parasympathetic innervation of the iris [125,126]. This may result in transient pupil dilation and attenuation of the PLR by uptake of BTx into the parasympathetic ciliary ganglion or the parasympathetic neuromuscular junctions at the iris sphincter muscle [127]. There are a number of reports in the literature describing mydriasis with an attenuated PLR as a consequence of ingesting contaminated food [128], or following injection of BTx [129,130].

Organophosphates, a family of chemicals that includes nerve agents and pesticides, inhibit cholinesterase activity, resulting in increased levels of ACh at the nerve synapses; they thus act

as an indirect cholinergic agonist. Published studies by Dabisch et al. and others suggest that the majority of cholinesterase inhibition observed within the eye is a result of the nerve agent vapour acting directly on the ocular tissues, rather than distributing to the eye as a result of systemic absorption [131–133]. The localised increase in ACh leads to contraction of the pupillary sphincter muscle, resulting in dose-dependent miosis [132,134–136]. Miosis is a highly sensitive index of exposure and can occur at exposure levels below those that cause systemic effects [137,138]. In relevant animal models, the amounts of sarin and cyclosarin required to produce miosis were up to 30- and 135-fold lower, respectively, than the amounts required for lethality [139].

The PLR is also reduced following organophosphate exposure, as a result of developing tolerance to cholinergic agonists and desensitization of muscarinic ACh receptors within retinal tissue following prolonged exposure [135,140,141]. The threshold dose required to attenuate the PLR is similar to that required to produce miosis, but the duration of the response is very different [140].

Dabisch et al. [140] observed rapid miosis and attenuation of the PLR in a rodent model following a single low-dose soman vapour exposure, but while pupil size returned to normal after 48 h, the PLR took up to 10 days to fully recover. Similarly, exposure to dichlorvos vapour resulted in a dose-dependent transient miotic response in the guinea pig; however, a persistent enhanced pupillary response to light was observed [136]. The recovery of pupil size is attributed to desensitisation of the muscarinic receptors rather than reactivation of cholinesterases within the eye, which may take up to 6 days to recover. Consequently, the PLR is attenuated until muscarinic receptor function is regained [142]. In support of this, oximes, which reactivate acetylcholinesterase, had no effect on sarin-induced miosis in animal models. Moreover, tropicamide—a muscarinic receptor antagonist that competes with ACh for binding sites, preventing receptor desensitisation—rapidly increased pupil size and restored PLR [143]. However, organophosphates inactivate cholinesterases at both muscarinic and nicotinic receptor sites and paradoxical pupil dilation or mydriasis may occur in certain circumstances due to dominant nicotinic effects at the pre-ganglionic fibres of the sympathetic nervous system, resulting in increased innervation of the dilator muscle [144,145].

### 5.6. Response to Infection

An area of interest that currently remains unexplored is the response of the PLR to infection and the potential diagnostic value of pupillometry. The brain monitors and modulates immune status through both humoral and neural pathways [146,147]. Neuroendocrine responses control inflammation at the systemic level through the hypothalamic-pituitary-adrenal axis [148]. The first branch of this pathway, the vagus nerve, is activated either directly by cytokines (released from innate immune cells) or indirectly through the chemoreceptive cells located in the vagal paraganglia [149]. The release of pro-inflammatory cytokines needs to be carefully controlled, as excessive or uncontrolled release (also known as a “cytokine storm”) may contribute to the pathogenesis of infections, including the novel coronaviruses SARS and MERS [150–152], influenza [153], and Ebola [154], as well as potential bacterial biothreat agents such as *Burkholderia pseudomallei* [155] and *Yersinia pestis* [156].

Signals from the vagus afferent fibres eventually project to the *locus coeruleus* region of the brain. The *locus coeruleus* exerts a dual influence on the PLR, ultimately leading to pupil dilation [157,158]. Firstly, it contributes to the sympathetic outflow that innervates the pupillary dilator muscle. Secondly, it attenuates the parasympathetic outflow via inhibition of the EW nucleus. Furthermore, experimental models of infection—including sepsis [159–161], pneumococcal pneumonia [162], endotoxaemia [163,164], leptospirosis [165,166] and influenza A [167,168]—have also highlighted the significance of the cholinergic signalling pathway during infection. Changes to cholinergic signalling are likely to influence the PLR both directly, through ACh receptors located on iris sphincter muscles, and indirectly, through altered parasympathetic nervous system function. Therefore, measurement of the PLR using dynamic pupillometry may offer the potential to detect systemic changes in parasympathetic and sympathetic system function in response to infection and inflammation.

## 6. Limitations

Pupillometry shows promise as a non-invasive diagnostic technology for a wide range of conditions. However, there are a number of limitations that require consideration and further research is needed to enable translation into clinical settings. Firstly, PLR measurements can be influenced by the light stimuli used [6,169], sex [170], age [171,172] and iris colour [173]. Changes in pupil size are also observed in response to other stimuli, including spatial structure patterns [174,175], object nearness or accommodation reflex [10], and a variety of emotional and cognitive stressors [176,177]. Therefore, it is critical that standardised protocols be developed to enable the use of pupillometry as a diagnostic tool and limiting factors should be considered as covariates or exclusion criteria in PLR studies to enable inter-study comparisons [23].

Further research is also required to establish whether the observed changes in PLR associated with different disorders are sufficient in terms of specificity and sensitivity to be used diagnostically. However, the ease of use, non-invasive nature and low cost mean pupillometry is well-placed for inclusion in early diagnostic screening assessments and could complement other sources of information to identify individuals at risk who warrant further clinic investigations.

Furthermore, there are approaches that have been exploited in particular fields—such as the use of chromatic pupillometry to measure the response of different sub-types of photoreceptor, specifically ipRGCs, in diabetes [66] and glaucoma [14,64,65]—which could be applied to other conditions including neurodegenerative disorders.

## 7. Conclusions

The pupillary light reflex serves as a valuable indicator of autonomic nervous system function. Moreover, measurement of the reflex using dynamic pupillometry provides a quantitative, non-invasive tool, which may aid the diagnosis and clinical management of a wide range of clinical conditions, varying from neurodegenerative disease to exposure to toxic chemicals.

**Acknowledgments:** The authors would like to thank Philip Lees for his assistance in finalizing this manuscript.

**Conflicts of Interest:** The authors declare no conflict of interest.

## References

1. Hirata, Y.; Yamaji, K.; Sakai, H.; Usui, S. Function of the pupil in vision and information capacity of retinal image. *Syst. Comput. Jpn.* **2003**, *34*, 48–57. [[CrossRef](#)]
2. McDougal, D.H.; Gamlin, P.D. Autonomic control of the eye. *Compr. Physiol.* **2015**, *5*, 439–473. [[CrossRef](#)] [[PubMed](#)]
3. Girkin, C. Evaluation of the pupillary light response as an objective measure of visual function. *Ophthalmol. Clin. N. Am.* **2003**, *16*, 143–153. [[CrossRef](#)]
4. Loewenfeld, I.E. *The Pupil: Anatomy, Physiology, and Clinical Applications*, 2nd ed.; Butterworth-Heinemann: Boston, MA, USA, 1999.
5. Winn, B.; Whitaker, D.; Elliott, D.B.; Phillips, N.J. Factors affecting light-adapted pupil size in normal human subjects. *Investig. Ophthalmol. Vis. Sci.* **1994**, *35*, 1132–1137.
6. Adhikari, P.; Pearson, C.A.; Anderson, A.M.; Zele, A.J.; Feigl, B. Effect of age and refractive error on the melanopsin mediated post-illumination pupil response (PIPR). *Sci. Rep.* **2015**, *5*, 17610. [[CrossRef](#)] [[PubMed](#)]
7. Ellis, C.J. The pupillary light reflex in normal subjects. *Br. J. Ophthalmol.* **1981**, *65*, 754–759. [[CrossRef](#)] [[PubMed](#)]
8. Lowenstein, O.; Loewenfeld, I.E. The sleep-waking cycle and pupillary activity. *Ann. N. Y. Acad. Sci.* **1964**, *117*, 142–156. [[CrossRef](#)] [[PubMed](#)]
9. Bergamin, O.; Kardon, R.H. Latency of the pupil light reflex: Sample rate, stimulus intensity, and variation in normal subjects. *Investig. Ophthalmol. Vis. Sci.* **2003**, *44*, 1546–1554. [[CrossRef](#)]
10. Barbur, J. Learning from the pupil: Studies of basic mechanisms and clinical applications. In *The Visual Neurosciences*; MIT: Cambridge, MA, USA, 2004; pp. 641–656.

11. Kawasaki, A.; Kardon, R.H. Intrinsically photosensitive retinal ganglion cells. *J. Neuroophthalmol.* **2007**, *27*, 195–204. [[CrossRef](#)] [[PubMed](#)]
12. Joyce, D.S.; Feigl, B.; Zele, A.J. Melanopsin-mediated post-illumination pupil response in the peripheral retina. *J. Vis.* **2016**, *16*, 5. [[CrossRef](#)] [[PubMed](#)]
13. Kankipati, L.; Girkin, C.A.; Gamlin, P.D. Post-illumination pupil response in subjects without ocular disease. *Investig. Ophthalmol. Vis. Sci.* **2010**, *51*, 2764–2769. [[CrossRef](#)] [[PubMed](#)]
14. Adhikari, P.; Feigl, B.; Zele, A.J. Rhodopsin and melanopsin contributions to the early redilation phase of the post-illumination pupil response (PIPR). *PLoS ONE* **2016**, *11*, e0161175. [[CrossRef](#)] [[PubMed](#)]
15. Gamlin, P.D.; McDougal, D.H.; Pokorny, J.; Smith, V.C.; Yau, K.W.; Dacey, D.M. Human and macaque pupil responses driven by melanopsin-containing retinal ganglion cells. *Vis. Res.* **2007**, *47*, 946–954. [[CrossRef](#)] [[PubMed](#)]
16. Rosen, E.S.; Gore, C.L.; Taylor, D.; Chitkara, D.; Howes, F.; Kowalewski, E. Use of a digital infrared pupillometer to assess patient suitability for refractive surgery. *J. Cataract Refract. Surg.* **2002**, *28*, 1433–1438. [[CrossRef](#)]
17. Smith, G.T. Repeatability of the procyon p3000 pupillometer. *J. Refract. Surg.* **2011**, *27*, 11. [[CrossRef](#)] [[PubMed](#)]
18. Chen, J.W.; Vakil-Gilani, K.; Williamson, K.L.; Cecil, S. Infrared pupillometry, the Neurological Pupil index and unilateral pupillary dilation after traumatic brain injury: Implications for treatment paradigms. *Springerplus* **2014**, *3*, 548. [[CrossRef](#)] [[PubMed](#)]
19. De Souza, J.K.; Pinto, M.A.; Vieira, P.G.; Baron, J.; Tierra-Criollo, C.J. An open-source, FireWire camera-based, Labview-controlled image acquisition system for automated, dynamic pupillometry and blink detection. *Comput. Methods Programs Biomed.* **2013**, *112*, 607–623. [[CrossRef](#)] [[PubMed](#)]
20. Bremner, F.D. Pupillometric evaluation of the dynamics of the pupillary response to a brief light stimulus in healthy subjects. *Investig. Ophthalmol. Vis. Sci.* **2012**, *53*, 7343–7347. [[CrossRef](#)] [[PubMed](#)]
21. Nyström, P.; Falck-Ytter, T.; Gredebäck, G. The TimeStudio Project: An open source scientific workflow system for the behavioral and brain sciences. *Behav. Res. Methods* **2016**, *48*, 542–552. [[CrossRef](#)] [[PubMed](#)]
22. Keivanidou, A.; Fotiou, D.; Arnaoutoglou, C.; Arnaoutoglou, M.; Fotiou, F.; Karlovasitou, A. Evaluation of autonomic imbalance in patients with heart failure: A preliminary study of pupillomotor function. *Cardiol. J.* **2010**, *17*, 65–72. [[PubMed](#)]
23. Wang, Y.; Zekveld, A.A.; Naylor, G.; Ohlenforst, B.; Jansma, E.P.; Lorens, A.; Lunner, T.; Kramer, S.E. Parasympathetic nervous system dysfunction, as identified by pupil light reflex, and its possible connection to hearing impairment. *PLoS ONE* **2016**, *11*, e0153566. [[CrossRef](#)] [[PubMed](#)]
24. Cepko, C.L. The Determination of Rod and Cone Photoreceptor Fate. *Annu. Rev. Vis. Sci.* **2015**, *1*, 211–234. [[CrossRef](#)] [[PubMed](#)]
25. Lamb, T.D. Why rods and cones? *Eye* **2016**, *30*, 179–185. [[CrossRef](#)] [[PubMed](#)]
26. Kawamura, S.; Tachibanaki, S. Explaining the functional differences of rods versus cones. *Wiley Interdiscip. Rev. Membr. Transp. Signal* **2012**, *1*, 675–683. [[CrossRef](#)]
27. Diamond, J.S. Inhibitory Interneurons in the Retina: Types, Circuitry, and Function. *Annu. Rev. Vis. Sci.* **2017**, *3*, 1–24. [[CrossRef](#)] [[PubMed](#)]
28. Dacey, D.M.; Liao, H.W.; Peterson, B.B.; Robinson, F.R.; Smith, V.C.; Pokorny, J.; Yau, K.W.; Gamlin, P.D. Melanopsin-expressing ganglion cells in primate retina signal colour and irradiance and project to the LGN. *Nature* **2005**, *433*, 749–754. [[CrossRef](#)] [[PubMed](#)]
29. Liao, H.-W.; Ren, X.; Peterson, B.B.; Marshak, D.W.; Yau, K.-W.; Gamlin, P.D.; Dacey, D.M. Melanopsin-expressing ganglion cells on macaque and human retinas form two morphologically distinct populations. *J. Comp. Neurol.* **2016**, *524*, 2845–2872. [[CrossRef](#)] [[PubMed](#)]
30. Nasir-Ahmad, S.; Lee, S.C.S.; Martin, P.R.; Grünert, U. Melanopsin-expressing ganglion cells in human retina: Morphology, distribution, and synaptic connections. *J. Comp. Neurol.* **2017**, *10*. [[CrossRef](#)] [[PubMed](#)]
31. Berson, D.M.; Dunn, F.A.; Takao, M. Phototransduction by retinal ganglion cells that set the circadian clock. *Science* **2002**, *295*, 1070–1073. [[CrossRef](#)] [[PubMed](#)]
32. Barnard, A.R.; Hattar, S.; Hankins, M.W.; Lucas, R.J. Melanopsin regulates visual processing in the mouse retina. *Curr. Biol.* **2006**, *16*, 389–395. [[CrossRef](#)] [[PubMed](#)]
33. Hattar, S.; Liao, H.W.; Takao, M.; Berson, D.M.; Yau, K.W. Melanopsin-containing retinal ganglion cells: Architecture, projections, and intrinsic photosensitivity. *Science* **2002**, *295*, 1065–1070. [[CrossRef](#)] [[PubMed](#)]



34. Graham, D.M.; Wong, K.Y.; Shapiro, P.; Frederick, C.; Pattabiraman, K.; Berson, D.M. Melanopsin ganglion cells use a membrane-associated rhabdomic phototransduction cascade. *J. Neurophysiol.* **2008**, *99*, 2522–2532. [[CrossRef](#)] [[PubMed](#)]
35. Hartwick, A.T.; Bramley, J.R.; Yu, J.; Stevens, K.T.; Allen, C.N.; Baldrige, W.H.; Sollars, P.J.; Pickard, G.E. Light-evoked calcium responses of isolated melanopsin-expressing retinal ganglion cells. *J. Neurosci.* **2007**, *27*, 13468–13480. [[CrossRef](#)] [[PubMed](#)]
36. Sekaran, S.; Lall, G.S.; Ralphs, K.L.; Wolstenholme, A.J.; Lucas, R.J.; Foster, R.G.; Hankins, M.W. 2-Aminoethoxydiphenylborane is an acute inhibitor of directly photosensitive retinal ganglion cell activity in vitro and in vivo. *J. Neurosci.* **2007**, *27*, 3981–3986. [[CrossRef](#)] [[PubMed](#)]
37. Warren, E.J.; Allen, C.N.; Brown, R.L.; Robinson, D.W. The light-activated signaling pathway in SCN-projecting rat retinal ganglion cells. *Eur. J. Neurosci.* **2006**, *23*, 2477–2487. [[CrossRef](#)] [[PubMed](#)]
38. Markwell, E.L.; Feigl, B.; Zele, A.J. Intrinsically photosensitive melanopsin retinal ganglion cell contributions to the pupillary light reflex and circadian rhythm. *Clin. Exp. Optom.* **2010**, *93*, 137–149. [[CrossRef](#)] [[PubMed](#)]
39. Adhikari, P.; Zele, A.J.; Feigl, B. The post-illumination pupil response (PIPR). *Investig. Ophthalmol. Vis. Sci.* **2015**, *56*, 3838–3849. [[CrossRef](#)] [[PubMed](#)]
40. Fu, Y.; Yau, K.W. Phototransduction in mouse rods and cones. *Pflugers Arch. Eur. J. Physiol.* **2007**, *454*, 805–819. [[CrossRef](#)] [[PubMed](#)]
41. Hoyt, W.F.; Luis, O. The primate chiasm. Details of visual fiber organization studied by silver impregnation techniques. *Arch. Ophthalmol.* **1963**, *70*, 69–85. [[CrossRef](#)] [[PubMed](#)]
42. Kozicz, T.; Bittencourt, J.C.; May, P.J.; Reiner, A.; Gamlin, P.D.; Palkovits, M.; Horn, A.K.; Toledo, C.A.; Ryabinin, A.E. The Edinger-Westphal nucleus: A historical, structural, and functional perspective on a dichotomous terminology. *J. Comp. Neurol.* **2011**, *519*, 1413–1434. [[CrossRef](#)] [[PubMed](#)]
43. Remington, L.A. *Clinical Anatomy of the Visual System*; Elsevier Health Sciences: Amsterdam, The Netherlands, 2011; 303p.
44. Kardon, R.; Anderson, S.C.; Damarjian, T.G.; Grace, E.M.; Stone, E.; Kawasaki, A. Chromatic pupillometry in patients with retinitis pigmentosa. *Ophthalmology* **2011**, *118*, 376–381. [[CrossRef](#)] [[PubMed](#)]
45. Johnson, L.N.; Hill, R.A.; Bartholomew, M.J. Correlation of afferent pupillary defect with visual field loss on automated perimetry. *Ophthalmology* **1988**, *95*, 1649–1655. [[CrossRef](#)]
46. Saari, M.; Koskela, P.; Masar, S.E. Effect of vehicle on pilocarpine-induced miosis. *Acta Ophthalmol.* **1978**, *56*, 496–503. [[CrossRef](#)]
47. Liu, J.H.; Dacus, A.C. Central cholinergic stimulation affects ocular functions through sympathetic pathways. *Investig. Ophthalmol. Vis. Sci.* **1990**, *31*, 1332–1338.
48. Hansen, M.S.; Sander, B.; Kawasaki, A.; Brøndsted, A.E.; Nissen, C. Prior light exposure enhances the pupil response to subsequent short wavelength (blue) light. *J. Clin. Exp. Ophthalmol.* **2011**, *2*, 1000152. [[CrossRef](#)]
49. Rubin, L.S. Pupillometric studies of alcoholism. *Int. J. Neurosci.* **1980**, *11*, 301–308. [[CrossRef](#)] [[PubMed](#)]
50. Rubin, L.S.; Gottheil, E.; Roberts, A.; Alterman, A.; Holstine, J. Effects of alcohol on autonomic reactivity in alcoholics. Pupillometric studies. III. *J. Stud. Alcohol* **1980**, *41*, 611–622. [[CrossRef](#)] [[PubMed](#)]
51. Roeklein, K.; Wong, P.; Ernecoff, N.; Miller, M.; Donofry, S.; Kamarck, M.; Wood-Vasey, W.M.; Franzen, P. The post illumination pupil response is reduced in seasonal affective disorder. *Psychiatry Res.* **2013**, *210*, 150–158. [[CrossRef](#)] [[PubMed](#)]
52. Bär, K.J.; Boettger, M.K.; Schulz, S.; Harzendorf, C.; Agelink, M.W.; Yeragani, V.K.; Chokka, P.; Voss, A. The interaction between pupil function and cardiovascular regulation in patients with acute schizophrenia. *Clin. Neurophysiol.* **2008**, *119*, 2209–2213. [[CrossRef](#)] [[PubMed](#)]
53. Bakes, A.; Bradshaw, C.M.; Szabadi, E. Attenuation of the pupillary light reflex in anxious patients. *Br. J. Clin. Pharmacol.* **1990**, *30*, 377–381. [[CrossRef](#)] [[PubMed](#)]
54. Bittner, D.M.; Wieseler, I.; Wilhelm, H.; Riepe, M.W.; Müller, N.G. Repetitive pupil light reflex: Potential marker in Alzheimer’s disease? *J. Alzheimer Dis.* **2014**, *42*, 1469–1477.
55. Fotiou, F.; Fountoulakis, K.N.; Tsolaki, M.; Goulas, A.; Palikaras, A. Changes in pupil reaction to light in Alzheimer’s disease patients: A preliminary report. *Int. J. Psychophysiol.* **2000**, *37*, 111–120. [[CrossRef](#)]
56. Tales, A.; Troscianko, T.; Lush, D.; Haworth, J.; Wilcock, G.K.; Butler, S.R. The pupillary light reflex in aging and Alzheimer’s disease. *Aging* **2001**, *13*, 473–478. [[PubMed](#)]

57. Fotiou, D.F.; Stergiou, V.; Tsiptsios, D.; Lithari, C.; Nakou, M.; Karlovasitou, A. Cholinergic deficiency in Alzheimer's and Parkinson's disease: Evaluation with pupillometry. *Int. J. Psychophysiol.* **2009**, *73*, 143–149. [[CrossRef](#)] [[PubMed](#)]
58. Giza, E.; Fotiou, D.; Bostantjopoulou, S.; Katsarou, Z.; Karlovasitou, A. Pupil light reflex in Parkinson's disease: Evaluation with pupillometry. *Int. J. Neurosci.* **2011**, *121*, 37–43. [[CrossRef](#)] [[PubMed](#)]
59. Micieli, G.; Tassorelli, C.; Martignoni, E.; Pacchetti, C.; Bruggi, P.; Magri, M.; Nappi, G. Disordered pupil reactivity in Parkinson's disease. *Clin. Auton. Res.* **1991**, *1*, 55–58. [[CrossRef](#)] [[PubMed](#)]
60. Stergiou, V.; Fotiou, D.; Tsiptsios, D.; Haidich, B.; Nakou, M.; Giantselidis, C.; Karlovasitou, A. Pupillometric findings in patients with Parkinson's disease and cognitive disorder. *Int. J. Psychophysiol.* **2009**, *72*, 97–101. [[CrossRef](#)] [[PubMed](#)]
61. Fan, X.; Miles, J.H.; Takahashi, N.; Yao, G. Abnormal transient pupillary light reflex in individuals with autism spectrum disorders. *J. Autism Dev. Disord.* **2009**, *39*, 1499–1508. [[CrossRef](#)] [[PubMed](#)]
62. Rubin, L.S. Patterns of pupillary dilatation and constriction in psychotic adults and autistic children. *J. Nerv. Ment. Dis.* **1961**, *133*, 130–142. [[CrossRef](#)] [[PubMed](#)]
63. Kankipati, L.; Girkin, C.A.; Gamlin, P.D. The post-illumination pupil response is reduced in glaucoma patients. *Investig. Ophthalmol. Vis. Sci.* **2011**, *52*, 2287–2292. [[CrossRef](#)] [[PubMed](#)]
64. Feigl, B.; Mattes, D.; Thomas, R.; Zele, A.J. Intrinsically photosensitive (melanopsin) retinal ganglion cell function in glaucoma. *Investig. Ophthalmol. Vis. Sci.* **2011**, *52*, 4362–4367. [[CrossRef](#)] [[PubMed](#)]
65. Nissen, C.; Sander, B.; Milea, D.; Kolko, M.; Herbst, K.; Hamard, P.; Lund-Andersen, H. Monochromatic pupillometry in unilateral glaucoma discloses no adaptive changes subserved by the ipRGCs. *Front. Neurol.* **2014**, *5*, 15. [[CrossRef](#)] [[PubMed](#)]
66. Feigl, B.; Zele, A.J.; Fader, S.M.; Howes, A.N.; Hughes, C.E.; Jones, K.A.; Jones, R. The post-illumination pupil response of melanopsin-expressing intrinsically photosensitive retinal ganglion cells in diabetes. *Acta Ophthalmol.* **2012**, *90*, e230–e234. [[CrossRef](#)] [[PubMed](#)]
67. Dütsch, M.; Marthol, H.; Michelson, G.; Neundörfer, B.; Hilz, M.J. Pupillography refines the diagnosis of diabetic autonomic neuropathy. *J. Neurol. Sci.* **2004**, *222*, 75–81. [[CrossRef](#)] [[PubMed](#)]
68. Ferrari, G.L.; Marques, J.L.; Gandhi, R.A.; Heller, S.R.; Schneider, F.K.; Tesfaye, S.; Gamba, H.R. Using dynamic pupillometry as a simple screening tool to detect autonomic neuropathy in patients with diabetes: A pilot study. *Biomed. Eng. Online* **2010**, *9*, 26. [[CrossRef](#)] [[PubMed](#)]
69. Kuroda, N.; Taniguchi, H.; Baba, S.; Yamamoto, M. The pupillary light reflex in borderline diabetics. *J. Int. Med. Res.* **1989**, *17*, 205–211. [[CrossRef](#)] [[PubMed](#)]
70. Yuan, D.; Spaeth, E.B.; Vernino, S.; Muppidi, S. Disproportionate pupillary involvement in diabetic autonomic neuropathy. *Clin. Auton. Res.* **2014**, *24*, 305–309. [[CrossRef](#)] [[PubMed](#)]
71. Dhakal, L.P.; Sen, A.; Stanko, C.M.; Rawal, B.; Heckman, M.G.; Hoyne, J.B.; Dimberg, E.L.; Freeman, M.L.; Ng, L.K.; Rabinstein, A.A.; et al. Early Absent Pupillary Light Reflexes After Cardiac Arrest in Patients Treated with Therapeutic Hypothermia. *Ther. Hypothermia Temp. Manag.* **2016**, *6*, 116–121. [[CrossRef](#)] [[PubMed](#)]
72. Fotiou, D.F.; Brozou, C.G.; Haidich, A.B.; Tsiptsios, D.; Nakou, M.; Kabitsi, A.; Giantselidis, C.; Fotiou, F. Pupil reaction to light in Alzheimer's disease: Evaluation of pupil size changes and mobility. *Aging Clin. Exp. Res.* **2007**, *19*, 364–371. [[CrossRef](#)] [[PubMed](#)]
73. Granholm, E.; Morris, S.; Galasko, D.; Shults, C.; Rogers, E.; Vukov, B. Tropicamide effects on pupil size and pupillary light reflexes in Alzheimer's and Parkinson's disease. *Int. J. Psychophysiol.* **2003**, *47*, 95–115. [[CrossRef](#)]
74. Prettyman, R.; Bitsios, P.; Szabadi, E. Altered pupillary size and darkness and light reflexes in Alzheimer's disease. *J. Neurol. Neurosurg. Psychiatry* **1997**, *62*, 665–668. [[CrossRef](#)] [[PubMed](#)]
75. Giza, E.; Fotiou, D.; Bostantjopoulou, S.; Katsarou, Z.; Gerasimou, G.; Gotzamani-Psarrakou, A.; Karlovasitou, A. Pupillometry and 123I-DaTSCAN imaging in Parkinson's disease: A comparison study. *Int. J. Neurosci.* **2012**, *122*, 26–34. [[CrossRef](#)] [[PubMed](#)]
76. Ferrario, E.; Molaschi, M.; Villa, L.; Varetto, O.; Bogetto, C.; Nuzzi, R. Is videopupillography useful in the diagnosis of Alzheimer's disease? *Neurology* **1998**, *50*, 642–644. [[CrossRef](#)] [[PubMed](#)]
77. Park, J.C.; McAnany, J.J. Effect of stimulus size and luminance on the rod-, cone-, and melanopsin-mediated pupillary light reflex. *J. Vis.* **2015**, *15*, 13. [[CrossRef](#)] [[PubMed](#)]

78. Yamaji, K.; Hirata, Y.; Usui, S. A method for monitoring autonomic nervous activity by pupillary flash response. *Syst. Comput. Jpn.* **2000**, *31*, 22–31. [[CrossRef](#)]
79. Chesnut, R.M.; Gautille, T.; Blunt, B.A.; Klauber, M.R.; Marshall, L.E. The localizing value of asymmetry in pupillary size in severe head injury: Relation to lesion type and location. *Neurosurgery* **1994**, *34*, 840–845. [[CrossRef](#)] [[PubMed](#)]
80. Park, J.C.; Moss, H.E.; McAnany, J.J. The Pupillary Light Reflex in Idiopathic Intracranial Hypertension. *Investig. Ophthalmol. Vis. Sci.* **2016**, *57*, 23–29. [[CrossRef](#)]
81. Taylor, W.R.; Chen, J.W.; Meltzer, H.; Gennarelli, T.A.; Kelbch, C.; Knowlton, S.; Richardson, J.; Lutch, M.J.; Farin, A.; Hulst, K.N.; et al. Quantitative pupillometry, a new technology: Normative data and preliminary observations in patients with acute head injury. *J. Neurosurg.* **2003**, *98*, 205–213. [[CrossRef](#)] [[PubMed](#)]
82. Chen, J.W.; Gombart, Z.J.; Rogers, S.; Gardiner, S.K.; Cecil, S.; Bullock, R.M. Pupillary reactivity as an early indicator of increased intracranial pressure: The introduction of the Neurological Pupil index. *Surg. Neurol. Int.* **2011**, *2*, 82. [[CrossRef](#)] [[PubMed](#)]
83. Morris, G.F.; Juul, N.; Marshall, S.B.; Benedict, B.; Marshall, L.F. Neurological deterioration as a potential alternative endpoint in human clinical trials of experimental pharmacological agents for treatment of severe traumatic brain injuries. *Neurosurgery* **1998**, *43*, 1369–1372. [[CrossRef](#)] [[PubMed](#)]
84. Meeker, M.; Du, R.; Bacchetti, P.; Privitera, C.M.; Larson, M.D.; Holland, M.C.; Manley, G. Pupil examination: Validity and clinical utility of an automated pupillometer. *J. Neurosci. Nurs.* **2005**, *37*, 34–40. [[CrossRef](#)] [[PubMed](#)]
85. Meyer, S.; Gibb, T.; Jurkovich, G.J. Evaluation and significance of the pupillary light reflex in trauma patients. *Ann. Emerg. Med.* **1993**, *22*, 1052–1057. [[CrossRef](#)]
86. Couret, D.; Boumaza, D.; Grisotto, C.; Triglia, T.; Pellegrini, L.; Ocquidant, P.; Bruder, N.J.; Velly, L.J. Reliability of standard pupillometry practice in neurocritical care: An observational, double-blinded study. *Crit. Care* **2016**, *20*, 99. [[CrossRef](#)] [[PubMed](#)]
87. Larson, M.D.; Muhiudeen, I. Pupillometric analysis of the ‘absent light reflex’. *Arch. Neurol.* **1995**, *52*, 369–372. [[CrossRef](#)] [[PubMed](#)]
88. Olson, D.M.; Stutzman, S.; Saju, C.; Wilson, M.; Zhao, W.; Aiyagari, V. Interrater Reliability of Pupillary Assessments. *Neurocrit. Care* **2016**, *24*, 251–257. [[CrossRef](#)] [[PubMed](#)]
89. Chang, D.S.; Boland, M.V.; Arora, K.S.; Supakontanasan, W.; Chen, B.B.; Friedman, D.S. Symmetry of the pupillary light reflex and its relationship to retinal nerve fiber layer thickness and visual field defect. *Investig. Ophthalmol. Vis. Sci.* **2013**, *54*, 5596–5601. [[CrossRef](#)] [[PubMed](#)]
90. Suys, T.; Bouzat, P.; Marques-Vidal, P.; Sala, N.; Payen, J.F.; Rossetti, A.O.; Oddo, M. Automated quantitative pupillometry for the prognostication of coma after cardiac arrest. *Neurocrit. Care* **2014**, *21*, 300–308. [[CrossRef](#)] [[PubMed](#)]
91. Heimburger, D.; Durand, M.; Gaide-Chevronnay, L.; Dessertaine, G.; Moury, P.H.; Bouzat, P.; Albaladejo, P.; Payen, J.F. Quantitative pupillometry and transcranial Doppler measurements in patients treated with hypothermia after cardiac arrest. *Resuscitation* **2016**, *103*, 88–93. [[CrossRef](#)] [[PubMed](#)]
92. Sokol, D.K.; Dunn, D.W.; Edwards-Brown, M.; Feinberg, J. Hydrogen proton magnetic resonance spectroscopy in autism: Preliminary evidence of elevated choline/creatine ratio. *J. Child Neurol.* **2002**, *17*, 245–249. [[CrossRef](#)] [[PubMed](#)]
93. Lee, M.; Martin-Ruiz, C.; Graham, A.; Court, J.; Jaros, E.; Perry, R.; Iversen, P.; Bauman, M.; Perry, E. Nicotinic receptor abnormalities in the cerebellar cortex in autism. *Brain* **2002**, *125*, 1483–1495. [[CrossRef](#)] [[PubMed](#)]
94. Perry, E.K.; Lee, M.L.; Martin-Ruiz, C.M.; Court, J.A.; Volsen, S.G.; Merrit, J.; Folly, E.; Iversen, P.E.; Bauman, M.L.; Perry, R.H.; et al. Cholinergic activity in autism: Abnormalities in the cerebral cortex and basal forebrain. *Am. J. Psychiatry* **2001**, *158*, 1058–1066. [[CrossRef](#)] [[PubMed](#)]
95. Karvat, G.; Kimchi, T. Acetylcholine elevation relieves cognitive rigidity and social deficiency in a mouse model of autism. *Neuropsychopharmacology* **2014**, *39*, 831–840. [[CrossRef](#)] [[PubMed](#)]
96. McTighe, S.M.; Neal, S.J.; Lin, Q.; Hughes, Z.A.; Smith, D.G. The BTBR mouse model of autism spectrum disorders has learning and attentional impairments and alterations in acetylcholine and kynurenic acid in prefrontal cortex. *PLoS ONE* **2013**, *8*, e62189. [[CrossRef](#)] [[PubMed](#)]
97. Leblond, C.S.; Heinrich, J.; Delorme, R.; Proepper, C.; Betancur, C.; Huguet, G.; Konyukh, M.; Chaste, P.; Ey, E.; Rastam, M.; et al. Genetic and functional analyses of SHANK2 mutations suggest a multiple hit model of autism spectrum disorders. *PLoS Genet.* **2012**, *8*, e1002521. [[CrossRef](#)] [[PubMed](#)]

98. Daluwatte, C.; Miles, J.H.; Sun, J.; Yao, G. Association between pupillary light reflex and sensory behaviors in children with autism spectrum disorders. *Res. Dev. Disabil.* **2015**, *37*, 209–215. [[CrossRef](#)] [[PubMed](#)]
99. Daluwatte, C.; Miles, J.H.; Christ, S.E.; Beversdorf, D.Q.; Takahashi, T.N.; Yao, G. Atypical pupillary light reflex and heart rate variability in children with autism spectrum disorder. *J. Autism Dev. Disord.* **2013**, *43*, 1910–1925. [[CrossRef](#)] [[PubMed](#)]
100. Nyström, P.; Gredebäck, G.; Bölte, S.; Falck-Ytter, T.; EASE Team. Hypersensitive pupillary light reflex in infants at risk for autism. *Mol. Autism* **2015**, *6*, 10. [[CrossRef](#)] [[PubMed](#)]
101. Dockstader, C.; Gaetz, W.; Rockel, C.; Mabbott, D.J. White matter maturation in visual and motor areas predicts the latency of visual activation in children. *Hum. Brain Mapp.* **2012**, *33*, 179–191. [[CrossRef](#)] [[PubMed](#)]
102. Ben Bashat, D.; Kronfeld-Duenias, V.; Zachor, D.A.; Ekstein, P.M.; Hendler, T.; Tarrasch, R.; Even, A.; Levy, Y.; Ben Sira, L. Accelerated maturation of white matter in young children with autism: A high b value DWI study. *Neuroimage* **2007**, *37*, 40–47. [[CrossRef](#)] [[PubMed](#)]
103. Courchesne, E. Abnormal early brain development in autism. *Mol. Psychiatry* **2002**, *7* (Suppl. 2), S21–S23. [[CrossRef](#)] [[PubMed](#)]
104. Courchesne, E.; Karns, C.M.; Davis, H.R.; Ziccardi, R.; Carper, R.A.; Tigue, Z.D.; Chisum, H.J.; Moses, P.; Pierce, K.; Lord, C.; et al. Unusual brain growth patterns in early life in patients with autistic disorder: An MRI study. *Neurology* **2001**, *57*, 245–254. [[CrossRef](#)] [[PubMed](#)]
105. Weinstein, M.; Ben-Sira, L.; Levy, Y.; Zachor, D.A.; Ben Itzhak, E.; Artzi, M.; Tarrasch, R.; Eksteine, P.M.; Hendler, T.; Ben Bashat, D. Abnormal white matter integrity in young children with autism. *Hum. Brain Mapp.* **2011**, *32*, 534–543. [[CrossRef](#)] [[PubMed](#)]
106. Wolff, J.J.; Gu, H.; Gerig, G.; Elison, J.T.; Styner, M.; Gouttard, S.; Botteron, K.N.; Dager, S.R.; Dawson, G.; Estes, A.M.; et al. Differences in white matter fiber tract development present from 6 to 24 months in infants with autism. *Am. J. Psychiatry* **2012**, *169*, 589–600. [[CrossRef](#)] [[PubMed](#)]
107. Vissers, M.E.; Cohen, M.X.; Geurts, H.M. Brain connectivity and high functioning autism: A promising path of research that needs refined models, methodological convergence, and stronger behavioral links. *Neurosci. Biobehav. Rev.* **2012**, *36*, 604–625. [[CrossRef](#)] [[PubMed](#)]
108. Courchesne, E.; Campbell, K.; Solso, S. Brain growth across the life span in autism: Age-specific changes in anatomical pathology. *Brain Res.* **2011**, *1380*, 138–145. [[CrossRef](#)] [[PubMed](#)]
109. DeVito, T.J.; Drost, D.J.; Neufeld, R.W.; Rajakumar, N.; Pavlosky, W.; Williamson, P.; Nicolson, R. Evidence for cortical dysfunction in autism: A proton magnetic resonance spectroscopic imaging study. *Biol. Psychiatry* **2007**, *61*, 465–473. [[CrossRef](#)] [[PubMed](#)]
110. Monticelli, F.; Priemer, F.; Hitzl, W.; Keller, T. Pupil function as an indicator for being under the influence of central nervous system-acting substances from a traffic-medicine perspective. *Med. Sci. Law* **2010**, *50*, 75–83. [[CrossRef](#)] [[PubMed](#)]
111. Monticelli, F.C.; Hitzl, W.; Priemer, F.; Preiss, U.; Kunz, S.N.; Keller, T. The potential of infrared pupillography in routine police traffic checks. *Rechtsmedizin* **2015**, *25*, 466–473. [[CrossRef](#)]
112. Monticelli, F.C.; Tutsch-Bauer, E.; Hitzl, W.; Keller, T. Pupil function as a parameter for assessing impairment of the central nervous system from a traffic-medicine perspective. *Leg. Med.* **2009**, *11* (Suppl. 1), S331–S332. [[CrossRef](#)] [[PubMed](#)]
113. Hartman, R.L.; Richman, J.E.; Hayes, C.E.; Huestis, M.A. Drug Recognition Expert (DRE) examination characteristics of cannabis impairment. *Accid. Anal. Prev.* **2016**, *92*, 219–229. [[CrossRef](#)] [[PubMed](#)]
114. Kosnoski, E.M.; Yolton, R.L.; Citek, K.; Hayes, C.E.; Evans, R.B. The Drug Evaluation Classification Program: Using ocular and other signs to detect drug intoxication. *J. Am. Optom. Assoc.* **1998**, *69*, 211–227. [[PubMed](#)]
115. Lobato-Rincón, L.L.; Cabanillas Campos, M.C.; Navarro-Valls, J.J.; Bonnin-Arias, C.; Chamorro, E.; Sánchez-Ramos Roda, C. Utility of dynamic pupillometry in alcohol testing on drivers. *Adicciones* **2013**, *25*, 137–145. [[CrossRef](#)] [[PubMed](#)]
116. Pickworth, W.B.; Rohrer, M.S.; Fant, R.V. Effects of abused drugs on psychomotor performance. *Exp. Clin. Psychopharmacol.* **1997**, *5*, 235–241. [[CrossRef](#)] [[PubMed](#)]
117. Tennant, F. The rapid eye test to detect drug abuse. *Postgrad. Med.* **1988**, *84*, 108–114. [[CrossRef](#)] [[PubMed](#)]
118. Sagawa, Y.; Kondo, H.; Matsubuchi, N.; Takemura, T.; Kanayama, H.; Kaneko, Y.; Kanbayashi, T.; Hishikawa, Y.; Shimizu, T. Alcohol has a dose-related effect on parasympathetic nerve activity during sleep. *Alcohol. Clin. Exp. Res.* **2011**, *35*, 2093–2100. [[CrossRef](#)] [[PubMed](#)]



119. Jochum, T.; Hoyme, J.; Schulz, S.; Weißenfels, M.; Voss, A.; Bär, K.J. Diverse autonomic regulation of pupillary function and the cardiovascular system during alcohol withdrawal. *Drug Alcohol Depend.* **2016**, *159*, 142–151. [[CrossRef](#)] [[PubMed](#)]
120. Engberg, G.; Hajós, M. Alcohol withdrawal reaction as a result of adaptive changes of excitatory amino acid receptors. *Naunyn Schmiedeberg Arch. Pharmacol.* **1992**, *346*, 437–441. [[CrossRef](#)]
121. Knapp, D.J.; Duncan, G.E.; Crews, F.T.; Breese, G.R. Induction of Fos-like proteins and ultrasonic vocalizations during ethanol withdrawal: Further evidence for withdrawal-induced anxiety. *Alcohol. Clin. Exp. Res.* **1998**, *22*, 481–493. [[CrossRef](#)] [[PubMed](#)]
122. Fant, R.V.; Heishman, S.J.; Bunker, E.B.; Pickworth, W.B. Acute and residual effects of marijuana in humans. *Pharmacol. Biochem. Behav.* **1998**, *60*, 777–784. [[CrossRef](#)]
123. Hysek, C.M.; Liechti, M.E. Effects of MDMA alone and after pretreatment with reboxetine, duloxetine, clonidine, carvedilol, and doxazosin on pupillary light reflex. *Psychopharmacology* **2012**, *224*, 363–376. [[CrossRef](#)] [[PubMed](#)]
124. Hepler, R.S.; Frank, I.M.; Ungerleider, J.T. Pupillary constriction after marijuana smoking. *Am. J. Ophthalmol.* **1972**, *74*, 1185–1190. [[CrossRef](#)]
125. Burgen, A.S.; Dickens, F.; Zatman, L.J. The action of botulinum toxin on the neuro-muscular junction. *J. Physiol.* **1949**, *109*, 10–24. [[CrossRef](#)] [[PubMed](#)]
126. Sellin, L.C. The pharmacological mechanism of botulism. *Trends Pharmacol. Sci.* **1985**, *6*, 80–82. [[CrossRef](#)]
127. Hemmerdinger, C.; Srinivasan, S.; Marsh, I.B. Reversible pupillary dilation following botulinum toxin injection to the lateral rectus. *Eye* **2006**, *20*, 1478–1479. [[CrossRef](#)] [[PubMed](#)]
128. Penas, S.C.; Faria, O.M.; Serrão, R.; Capão-Filipe, J.A.; Mota-Miranda, A.; Falcão-Reis, F. Ophthalmic manifestations in 18 patients with botulism diagnosed in Porto, Portugal between 1998 and 2003. *J. Neuroophthalmol.* **2005**, *25*, 262–267. [[CrossRef](#)] [[PubMed](#)]
129. Akkaya, S.; Kökcen, H.K.; Atakan, T. Unilateral transient mydriasis and ptosis after botulinum toxin injection for a cosmetic procedure. *Clin. Ophthalmol.* **2015**, *9*, 313–315. [[CrossRef](#)] [[PubMed](#)]
130. Christiansen, S.P.; Chandler, D.L.; Lee, K.A.; Superstein, R.; de Alba Campomanes, A.; Bothun, E.D.; Morin, J.; Wallace, D.K.; Kraker, R.T. Pediatric Eye Disease Investigator Group. Tonic pupil after botulinum toxin-A injection for treatment of esotropia in children. *J. AAPOS* **2016**, *20*, 78–81. [[CrossRef](#)] [[PubMed](#)]
131. Dabisch, P.A.; Burnett, D.C.; Miller, D.B.; Jakubowski, E.M.; Muse, W.T.; Forster, J.S.; Scotto, J.A.; Jarvis, J.R.; Davis, E.A.; Hulet, S.W.; et al. Tolerance to the miotic effect of sarin vapor in rats after multiple low-level exposures. *J. Ocul. Pharmacol. Ther.* **2005**, *21*, 182–195. [[CrossRef](#)] [[PubMed](#)]
132. Dabisch, P.A.; Miller, D.B.; Reutter, S.A.; Mioduszewski, R.J.; Thomson, S.A. Miotic tolerance to sarin vapor exposure: Role of the sympathetic and parasympathetic nervous systems. *Toxicol. Sci.* **2005**, *85*, 1041–1047. [[CrossRef](#)] [[PubMed](#)]
133. Yanagisawa, N.; Morita, H.; Nakajima, T. Sarin experiences in Japan: Acute toxicity and long-term effects. *J. Neurol. Sci.* **2006**, *249*, 76–85. [[CrossRef](#)] [[PubMed](#)]
134. Rengstorff, R.H. Vision and ocular changes following accidental exposure to organophosphates. *J. Appl. Toxicol.* **1994**, *14*, 115–118. [[CrossRef](#)] [[PubMed](#)]
135. Smith, S.A.; Smith, S.E. Factors determining the potency of cholinomimetic miotic drugs and their effect upon the light reflex in man. *Br. J. Clin. Pharmacol.* **1978**, *6*, 149–153. [[CrossRef](#)] [[PubMed](#)]
136. Taylor, J.T.; Davis, E.; Dabisch, P.; Horsmon, M.; Li, M.; Mioduszewski, R. Alterations in autonomic function in the guinea pig eye following exposure to dichlorvos vapor. *J. Ocul. Pharmacol. Ther.* **2008**, *24*, 473–479. [[CrossRef](#)] [[PubMed](#)]
137. Genovese, R.F.; Benton, B.J.; Oubre, J.L.; Fleming, P.J.; Jakubowski, E.M.; Mioduszewski, R.J. Evaluation of miosis, behavior and cholinesterase inhibition from low-level, whole-body vapor exposure to soman in African green monkeys (*Chlorocebus sabeus*). *J. Med. Primatol.* **2010**, *39*, 318–327. [[CrossRef](#)] [[PubMed](#)]
138. Nozaki, H.; Hori, S.; Shinozawa, Y.; Fujishima, S.; Takuma, K.; Kimura, H.; Suzuki, M.; Aikawa, N. Relationship between pupil size and acetylcholinesterase activity in patients exposed to sarin vapor. *Intensive Care Med.* **1997**, *23*, 1005–1007. [[CrossRef](#)] [[PubMed](#)]
139. Hulet, S.W.; Sommerville, D.R.; Crosier, R.B.; Dabisch, P.A.; Miller, D.B.; Benton, B.J.; Forster, J.S.; Scotto, J.A.; Jarvis, J.R.; Krauthauser, C.; et al. Comparison of low-level sarin and cyclosarin vapor exposure on pupil size of the Gottingen minipig: Effects of exposure concentration and duration. *Inhal. Toxicol.* **2006**, *18*, 143–153. [[CrossRef](#)] [[PubMed](#)]



140. Dabisch, P.A.; Horsmon, M.S.; Taylor, J.T.; Muse, W.T.; Miller, D.B.; Sommerville, D.R.; Mioduszezski, R.J.; Thomson, S. Gender difference in the mitotic potency of soman vapor in rats. *Cutan. Ocul. Toxicol.* **2008**, *27*, 123–133. [[CrossRef](#)] [[PubMed](#)]
141. Tandon, P.; Padilla, S.; Barone, S., Jr.; Pope, C.N.; Tilson, H.A. Fenthion produces a persistent decrease in muscarinic receptor function in the adult rat retina. *Toxicol. Appl. Pharmacol.* **1994**, *125*, 271–280. [[CrossRef](#)] [[PubMed](#)]
142. Dabisch, P.A.; Horsmon, M.S.; Muse, W.T.; Mioduszezski, R.J.; Thomson, S. Muscarinic receptor dysfunction induced by exposure to low levels of soman vapor. *Toxicol. Sci.* **2007**, *100*, 281–289. [[CrossRef](#)] [[PubMed](#)]
143. Gore, A.; Bloch-Shilderman, E.; Egoz, I.; Turetz, J.; Brandeis, R. Efficacy assessment of a combined anticholinergic and oxime treatment against topical sarin-induced miosis and visual impairment in rats. *Br. J. Pharmacol.* **2014**, *171*, 2364–2374. [[CrossRef](#)] [[PubMed](#)]
144. Lotti, M. Clinical Toxicology of Anticholinesterase Agents in Humans. In *Handbook of Pesticide Toxicology*; Elsevier: Amsterdam, The Netherlands, 2001; pp. 1043–1085.
145. Shirakawa, S.; Ishikawa, S.; Miyata, M.; Rea, W.J.; Johnson, A.R. A pupillographical study on the presence of organochlorine pesticides in autonomic nerve disturbance. *Nippon Ganka Gakkai Zasshi* **1990**, *94*, 418–423. [[PubMed](#)]
146. Pavlov, V.A.; Wang, H.; Czura, C.J.; Friedman, S.G.; Tracey, K.J. The cholinergic anti-inflammatory pathway: A missing link in neuroimmunomodulation. *Mol. Med.* **2003**, *9*, 125–134. [[CrossRef](#)] [[PubMed](#)]
147. Tracey, K.J. The inflammatory reflex. *Nature* **2002**, *420*, 853–859. [[CrossRef](#)] [[PubMed](#)]
148. Sternberg, E.M. Neural regulation of innate immunity: A coordinated nonspecific host response to pathogens. *Nat. Rev. Immunol.* **2006**, *6*, 318–328. [[CrossRef](#)] [[PubMed](#)]
149. Goehler, L.E.; Gaykema, R.P.; Hansen, M.K.; Anderson, K.; Maier, S.F.; Watkins, L.R. Vagal immune-to-brain communication: A visceral chemosensory pathway. *Auton. Neurosci. Basic Clin.* **2000**, *85*, 49–59. [[CrossRef](#)]
150. Channappanavar, R.; Perlman, S. Pathogenic human coronavirus infections: Causes and consequences of cytokine storm and immunopathology. *Semin. Immunopathol.* **2017**, *39*, 529–539. [[CrossRef](#)] [[PubMed](#)]
151. Huang, K.J.; Su, I.J.; Theron, M.; Wu, Y.C.; Lai, S.K.; Liu, C.C.; Lei, H.Y. An interferon-gamma-related cytokine storm in SARS patients. *J. Med. Virol.* **2005**, *75*, 185–194. [[CrossRef](#)] [[PubMed](#)]
152. Yiu, H.H.; Graham, A.L.; Stengel, R.F. Dynamics of a cytokine storm. *PLoS ONE* **2012**, *7*, e45027. [[CrossRef](#)] [[PubMed](#)]
153. Liu, Q.; Zhou, Y.H.; Yang, Z.Q. The cytokine storm of severe influenza and development of immunomodulatory therapy. *Cell. Mol. Immunol.* **2016**, *13*, 3–10. [[CrossRef](#)] [[PubMed](#)]
154. Mohamadzadeh, M.; Chen, L.; Schmaljohn, A.L. How Ebola and Marburg viruses battle the immune system. *Nat. Rev. Immunol.* **2007**, *7*, 556–567. [[CrossRef](#)] [[PubMed](#)]
155. Kessler, B.; Rinchai, D.; Kewcharoenwong, C.; Nithichanon, A.; Biggart, R.; Hawrylowicz, C.M.; Bancroft, G.J.; Lertmemongkolchai, G. Interleukin 10 inhibits pro-inflammatory cytokine responses and killing of *Burkholderia pseudomallei*. *Sci. Rep.* **2017**, *7*, 42791. [[CrossRef](#)] [[PubMed](#)]
156. Pechous, R.D.; Sivaraman, V.; Price, P.A.; Stasulli, N.M.; Goldman, W.E. Early host cell targets of *Yersinia pestis* during primary pneumonic plague. *PLoS Pathog.* **2013**, *9*, e1003679. [[CrossRef](#)] [[PubMed](#)]
157. Samuels, E.R.; Szabadi, E. Functional neuroanatomy of the noradrenergic locus coeruleus: Its roles in the regulation of arousal and autonomic function part II: Physiological and pharmacological manipulations and pathological alterations of locus coeruleus activity in humans. *Curr. Neuropharmacol.* **2008**, *6*, 254–285. [[CrossRef](#)] [[PubMed](#)]
158. Szabadi, E. Modulation of physiological reflexes by pain: Role of the locus coeruleus. *Front. Integr. Neurosci.* **2012**, *6*, 94. [[CrossRef](#)] [[PubMed](#)]
159. Song, X.M.; Li, J.G.; Wang, Y.L.; Hu, Z.F.; Zhou, Q.; Du, Z.H.; Jia, B.H. The protective effect of the cholinergic anti-inflammatory pathway against septic shock in rats. *Shock* **2008**, *30*, 468–472. [[CrossRef](#)] [[PubMed](#)]
160. Van Westerloo, D.J.; Giebelen, I.A.; Florquin, S.; Daalhuisen, J.; Bruno, M.J.; de Vos, A.F.; Tracey, K.J.; van der Poll, T. The cholinergic anti-inflammatory pathway regulates the host response during septic peritonitis. *J. Infect. Dis.* **2005**, *191*, 2138–2148. [[CrossRef](#)] [[PubMed](#)]
161. Wang, H.; Liao, H.; Ochani, M.; Justiniani, M.; Lin, X.; Yang, L.; Al-Abed, Y.; Wang, H.; Metz, C.; Miller, E.J.; et al. Cholinergic agonists inhibit HMGB1 release and improve survival in experimental sepsis. *Nat. Med.* **2004**, *10*, 1216–1221. [[CrossRef](#)] [[PubMed](#)]

162. Giebelen, I.A.; Leendertse, M.; Florquin, S.; van der Poll, T. Stimulation of acetylcholine receptors impairs host defence during pneumococcal pneumonia. *Eur. Respir. J.* **2009**, *33*, 375–381. [[CrossRef](#)] [[PubMed](#)]
163. Pavlov, V.A.; Parrish, W.R.; Rosas-Ballina, M.; Ochani, M.; Puerta, M.; Ochani, K.; Chavan, S.; Al-Abed, Y.; Tracey, K.J. Brain acetylcholinesterase activity controls systemic cytokine levels through the cholinergic anti-inflammatory pathway. *Brain Behav. Immun.* **2009**, *23*, 41–45. [[CrossRef](#)] [[PubMed](#)]
164. Pavlov, V.A.; Tracey, K.J. Controlling inflammation: The cholinergic anti-inflammatory pathway. *Biochem. Soc. Trans.* **2006**, *34*, 1037–1040. [[CrossRef](#)] [[PubMed](#)]
165. Rosas-Ballina, M.; Valdés-Ferrer, S.I.; Dancho, M.E.; Ochani, M.; Katz, D.; Cheng, K.F.; Olofsson, P.S.; Chavan, S.S.; Al-Abed, Y.; Tracey, K.J.; et al. Xanomeline suppresses excessive pro-inflammatory cytokine responses through neural signal-mediated pathways and improves survival in lethal inflammation. *Brain Behav. Immun.* **2015**, *44*, 19–27. [[CrossRef](#)] [[PubMed](#)]
166. Da Silva, C.B.; Wolkmer, P.; Da Silva, A.S.; Paim, F.C.; Tonin, A.A.; Castro, V.S.; Felin, D.V.; Schmatz, R.; Gonçalves, J.F.; Badke, M.R.; et al. Cholinesterases as markers of the inflammatory process in rats infected with *Leptospira interrogans* serovar Icterohaemorrhagiae. *J. Med. Microbiol.* **2012**, *61*, 278–284. [[CrossRef](#)] [[PubMed](#)]
167. Carr, M.J.; Goldie, R.G.; Henry, P.J. Influence of respiratory tract viral infection on endothelin-1-induced potentiation of cholinergic nerve-mediated contraction in mouse trachea. *Br. J. Pharmacol.* **1996**, *119*, 891–898. [[CrossRef](#)] [[PubMed](#)]
168. Ng, Y.P.; Lee, S.M.; Cheung, T.K.; Nicholls, J.M.; Peiris, J.S.; Ip, N.Y. Avian influenza H5N1 virus induces cytopathy and proinflammatory cytokine responses in human astrocytic and neuronal cell lines. *Neuroscience* **2010**, *168*, 613–623. [[CrossRef](#)] [[PubMed](#)]
169. Barbur, J.L.; Harlow, A.J.; Sahraie, A. Pupillary responses to stimulus structure, colour and movement. *Ophthalmic Physiol. Opt.* **1992**, *12*, 137–141. [[CrossRef](#)] [[PubMed](#)]
170. Fan, X.; Hearne, L.; Lei, B.; Miles, J.H.; Takahashi, N.; Yao, G. Weak gender effects on transient pupillary light reflex. *Auton. Neurosci. Basic Clin.* **2009**, *147*, 9–13. [[CrossRef](#)] [[PubMed](#)]
171. Fotiou, D.F.; Brozou, C.G.; Tsipsios, D.J.; Fotiou, A.; Kabitsi, A.; Nakou, M.; Giantselidis, C.; Goula, A. Effect of age on pupillary light reflex: Evaluation of pupil mobility for clinical practice and research. *Electromyogr. Clin. Neurophysiol.* **2007**, *47*, 11–22. [[PubMed](#)]
172. Straub, R.H.; Thies, U.; Kerp, L. The pupillary light reflex. 1. Age-dependent and age-independent parameters in normal subjects. *Ophthalmologica* **1992**, *204*, 134–142. [[CrossRef](#)] [[PubMed](#)]
173. Bergamin, O.; Schoetzau, A.; Sugimoto, K.; Zulauf, M. The influence of iris color on the pupillary light reflex. *Graefe Arch. Clin. Exp. Ophthalmol.* **1998**, *236*, 567–570. [[CrossRef](#)]
174. Slooter, J.; van Norren, D. Visual acuity measured with pupil responses to checkerboard stimuli. *Investig. Ophthalmol. Vis. Sci.* **1980**, *19*, 105–108.
175. Ukai, K. Spatial pattern as a stimulus to the pupillary system. *J. Opt. Soc. Am. A* **1985**, *2*, 1094–1100. [[CrossRef](#)] [[PubMed](#)]
176. Beatty, J. Task-evoked pupillary responses, processing load, and the structure of processing resources. *Psychol. Bull.* **1982**, *91*, 276–292. [[CrossRef](#)] [[PubMed](#)]
177. Newsome, D.A.; Loewenfeld, I.E. Iris mechanics. II. Influence of pupil size on details of iris structure. *Am. J. Ophthalmol.* **1971**, *71*, 553–573. [[CrossRef](#)]

